BJOS
Brazilian Journal of Oral Sciences

Volume 23
2024
e243907

Original Research

Influence of the X-ray source and the digital image receptor on the expression of halo artefacts around dental implants

Manuella Soussa Braga[1], Ana Maria de Almeida Ramos[1], Fernanda Coelho-Silva[2], Teresa Cristina Rangel Pereira[1], Sergio Lins de-Azevedo-Vaz[1,2*]

[1] Department of Clinical Dentistry, Federal University of Espírito Santo, Vitória, Espírito Santo, Brazil.

[2] Department of Oral Diagnosis, Division of Oral Radiology, Faculdade de Odontologia de Piracicaba (FOP), Universidade Estadual de Campinas (UNICAMP), Piracicaba, São Paulo, Brazil.

Objectives: To assess if different dental X-ray sources and receptors can improve the bone-to-implant interface image visualization by preventing halo artefact expression in terms of presence and magnitude. **Methods:** 144 digital periapical radiographs of eight titanium implants installed in two human jaws were obtained using two devices (high- and low-frequency X-ray sources) and two radiographic receptors (complementary solid metal oxide semiconductor sensor, and phosphor storage plate). Two evaluators assessed the presence or absence of halo on the left, right and apical surfaces of the implants. In surfaces with halo, the area was segmented and quantified to measure the magnitude of artefact using the Trainable Weka Segmentation plugin of the ImageJ software. Statistics comprised Cochran's Q, ANOVA, Kappa, and Intraclass Correlation tests (α = 5%). **Results:** Intra-examiner reproducibility was substantial and excellent. No surface showed statistically significant differences between the paired groups considering halo presence. 85 radiographs had at least one surface with halo, but the magnitude of halo did not vary considering the X-ray sources and radiographic receptors studied. **Conclusion:** Neither different X-ray sources nor radiographic receptor used in dentistry could improve the bone-to-implant interface image by preventing the presence or reducing the magnitude of halo artefacts.

Keywords: Artefacts. Dental implants. Radiography, dental, digital.

Corresponding author:
Sergio Lins de-Azevedo-Vaz
Department of Clinical Dentistry,
Federal University of Espírito Santo
1468th Marechal Campos Ave,
Maruípe, Vitória-ES, Brazil –
Zip code 29043-900
Phone/Fax: + 55 27 3335-7242.
E-mail: sergio.vaz@ufes.br

Editor: Dr. Altair A. Del Bel Cury

Received: July 7, 2023
Accepted: September 19, 2023

Introduction

The absence of peri-implant radiolucencies that may indicate flaws in osseointegration is one of the key criteria to establish the success of dental implants[1]. Despite their advantages when compared to radiographic films, digital periapical radiographs are usually associated with the occurrence of halo artefacts – also known as Uberschwinger artefact, and "blooming" or "burn out" phenomenon – which can simulate peri-implant radiolucencies[2-6]. The halo artefact appears as a radiolucent line around a metal or other high-density object. In dentistry, it can also mimic misfits at restoration margins and recurrent caries, which can lead to erroneous treatment decisions[4,7]. The halo artefact is associated with the use of sharpness filters and with the energetic parameters involved in X-ray production, such as kilovoltage-peak (kVp)[4-6]. It also can be associated to an overflow of energy that exceeds the receptor's limit range, making pixels in certain regions oversaturated, thus appearing "black" or "burned out" in the image[2].

Dental digital radiography can be obtained using the complementary metal-oxide semiconductor (CMOS) sensor, charged-coupled device (CCD) sensor and photostimulable phosphor plate (PSP). Although CMOS and CCD sensors have similar structures, the current production volume of CMOS is much higher than CCD for some advantages such as high-speed data transfer because each pixel is independently connected to the output, for example[8]. Furthermore, CMOS receptors are prone to a higher dispersion of radiation than PSP due to their bigger physical thickness associated to its plastic[9]. The dispersion of radiation is caused mainly by Compton scattering and can generate radiolucent artefacts in the digital image, such as the halo artefact[10,11].

High-frequency X-ray sources allow a better use of the consumed energy when compared to low-frequency sources, reducing exposure time and, consequently, generating a lower radiation dose to the patient[12,13]. In addition, for the same kVp and radiographic density settings, the images resulting from high-frequency devices have a lower contrast than those obtained with low-frequency devices. This could compensate for the sudden density difference between dental implant and surrounding alveolar bone by providing a more homogenous distribution of grey values, thus reducing the expression of halo artefacts[14].

Little is known regarding the outcomes of using high- and low-frequency X-ray sources, as well as different radiographic receptors currently used in dentistry (i.e.; CMOS and PSP), in halo artefact formation. Considering the available knowledge regarding these, we hypothesized that high-frequency devices with lower kVp and PSP receptor would reduce halo artefacts and, therefore, improve the radiographic image of the bone-to-implant interface, due to the longer contrast scale and decreased radiation scattering. To test our hypothesis, the aim of this study was to assess the influence of different X-ray sources (high and low frequency) and radiographic receptors (CMOS and PSP) on the expression of halo artefacts, in terms of presence and magnitude, in digital periapical radiographs of dental implants acquired with two kVp settings.

Methods

This was an *ex vivo* experimental study carried out after approval by the local Research Ethics Committee (protocol #05675718.8.0000.5060) and it is in accordance with the Helsinki Declaration.

Sample preparation

Four external hexagon titanium implants with 3.75 mm in diameter (TitamaxTi, Neodent, Curitiba/PR, Brazil) were placed in two partially edentulous dried human jaws. Thus, eight implants were inserted in the regions of first premolars and first molars on both sides. Following the manufacturer's recommendations, initially a spear-type drill (Neodent, Curitiba/PR, Brazil) was used in the milling sequence. Using the canal made by the drill as a guideline, the Titamax 2.0, pilot 2/3, and the Titamax 3.0 and 3.15 cylindrical drills (Neodent, Curitiba/PR, Brazil) were used, respectively. The installation was carried out under abundant irrigation with saline solution. In addition, the insertion of the implants followed the criteria of parallelism and long axis of the adjacent teeth, so that the implant neck was at the level of the alveolar ridge.

Image acquisition

The images were obtained using a high-frequency device (Focus™, 100-120 Hz, 60/70 kVp, 7 mA, Kavo, Tuusula, Finland) and a low-frequency device (Timex 70E, 50-60 Hz, 70 kVp, 7 mA, Gnatus, Ribeirão Preto, Brazil), with an exposure time of 0.2 seconds and a focus-receptor distance of 40 cm. The radiographs were obtained using 60 and 70 kVp in the high-frequency device. In addition, two image receptors were used: type 1, size 1 (23 x 39 mm) CMOS (Snapshot, Kavo, Tuusula, Finland); and type 1, size 2 (31 x 41 mm) PSP (VistaScan Mini Easy, Durr Dental, Beitigheim-Bissingen, Germany). Automatic application of filters by the software of the digital systems (Cliniview Kavo, Tuusula, Finland; Viewbox Studio, Durr Dental, Beitigheim-Bissingen, Germany) were disabled before images acquisition.

Since halo artefacts are absent when radiographic films are used, radiographic images were obtained under all study conditions using chemically processed radiographic films. Such radiographs were taken in order to verify the absence of gaps between the implant and the alveolar bone, which could produce peri-implant radiolucencies. This verification was done by the actual operator.

In order to standardize the images obtained, the periapical radiographs were performed by a single trained operator, using an acrylic device that allowed the image receptor to be parallel to each implant installed (Figure 1). Additionally, an acrylic plate of 20 mm thickness was used to simulate the attenuation of X radiation caused by the patient's soft tissues[15] (Figure 1). Considering the factors under study, six experimental groups were formed (Table 1). Since variations in the X-ray tube current could influence the results to be obtained, three digital radiographs per implant were performed to guarantee repetitions of the same experimental condition. Thus, a total of 144 radiographs were obtained (8 implants x 3 exposures x 6 experimental groups), stored as 32 bit .jpeg files. The images were then coded and randomized using Microsoft Excel (Microsoft®, Redmond, WA).

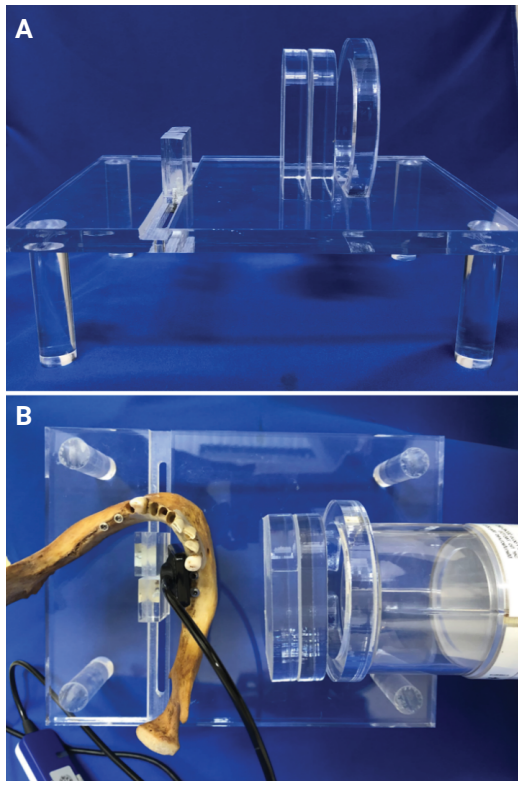

Figure 1. **1A.** Acrylic device used for image acquisition, with an acrylic plate of 20 mm thickness to mimic soft tissue attenuation. **1B.** Demonstration of the positioning of acrylic device, acrylic plate, dry mandible with implants, CMOS sensor and X-ray device.

Table 1. Experimental groups, according to X-ray devices, digital receptor and kilovoltage.

Groups	X-ray devices	Frequency	Receptor	Kilovoltage (kVp)	Paired Groups
A	Timex	Low	PSP	70	A and C
B		Low	CMOS	70	B and D
C	Focus	High	PSP	70	A and B
D		High	CMOS	70	C and D
E		High	PSP	60	E and F
F		High	CMOS	60	C and F
					D and F

kVp, kilovoltage peak; PSP, photostimulable phosphor plate; CMOS, Complementary Metal Oxide Semiconductor. Paired groups used for subjective analysis, according to X-ray source, type of receptor and kilovoltage.

Image evaluation

Two oral radiologists with at least four years of experience with digital radiographs evaluated the digital radiographs for halo presence/absence (subjective analysis), and one of them assessed the magnitude of halo (objective analysis). Both evaluations were performed in a dimly lit environment using an Asus SonicMaster AR5B225 notebook

(AsusTek Computer Inc, Taipei, Taiwan). They were allowed to use the zoom tool, but not brightness and contrast adjustments or filter application.

After training sessions conducted with images not included in the study, the evaluators initiated the subjective analysis using the Windows image viewer software (Microsoft®, Redmond, WA). To this end, they assessed each radiograph under consensus and answered whether a radiolucent halo around the dental implant (left, right and apical surfaces) was present or absent. Radiographs presenting a halo on at least one of the surfaces (Figure 2) were objectively assessed, so that the three surfaces were included.

The evaluator used the *Trainable Weka Segmentation* plugin of the ImageJ software (National Institutes of Health, Bethesda, MD, USA) for the objective analysis (Figure 2). This consisted of a semi-automatic segmentation of the halo artefact area in the bone-to-implant interface on the left, right and apical surfaces of each implant. First, the evaluator selected a region of interest (ROI) with dimensions of 3 mm width and 4 mm height, including the implant surfaces and the adjacent bone (Figure 3A). Then, the evaluator positioned classifiers of different sizes in areas of opposite densities: red classifiers in radiopaque areas – bone and implant surface; and green classifiers in radiolucent areas – halo artefact area (Figure 3B). The segmented artefact area was calculated using the ROI Manager tool and expressed in mm² (Figure 3C). This area represented the quantitative expression of the halo artefact magnitude. Thirty days after concluding the evaluations, the evaluators reassessed 20% of the sample to measure their reproducibility.

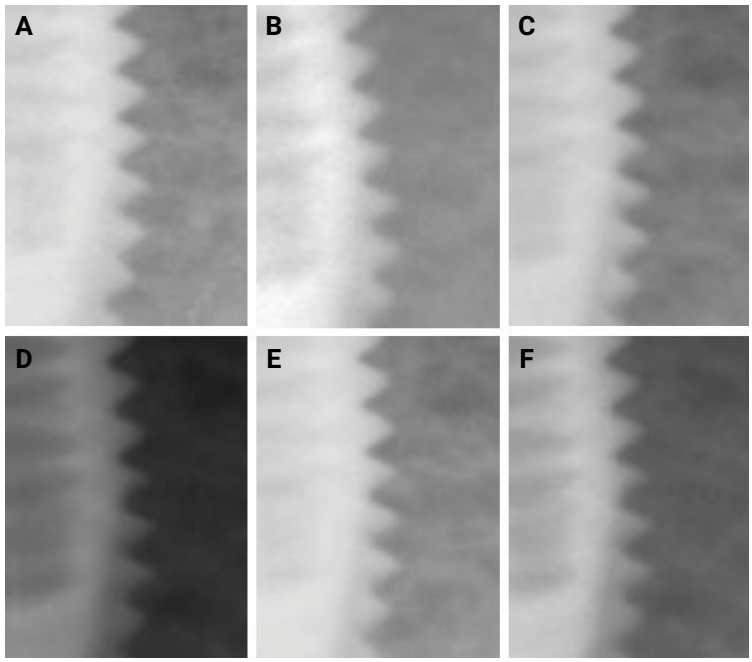

Figure 2. Examples of radiographs cropped at the right surface of the implants in which the halo artefact was considered present, according to the subjective analysis. **2A. Group A** – low frequency, PSP, 70 kVp. **2B. Group B** – low frequency, CMOS, 70 kVp. **2C. Group C** – high frequency, PSP, 70 kVp. **2D. Group D** – high frequency, CMOS, 70 kVp. **2E. Group E** – high frequency, PSP, 60 kVp. **2F. Group F** – high frequency, CMOS, 60 kVp.

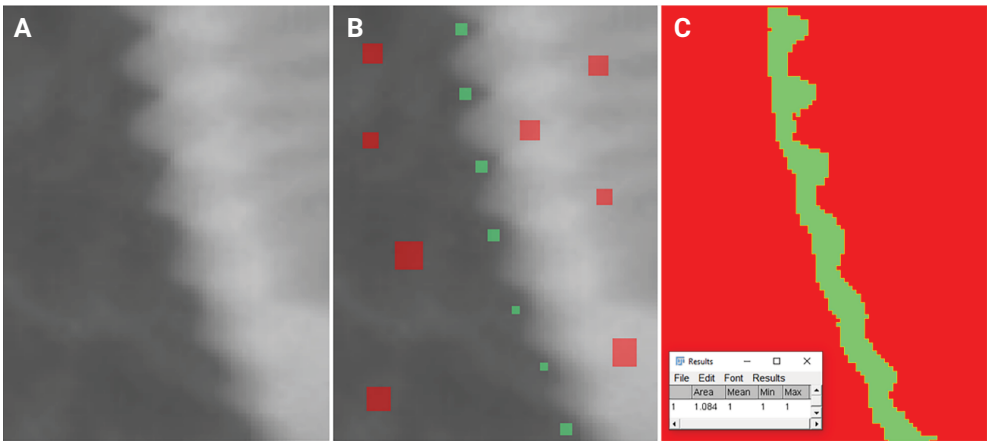

Figure 3. Steps of the semi-automatic segmentation process of the left surface of an implant using the *Trainable Weka Segmentation* plugin of the ImageJ software. **3A.** Selected region of interest (3 mm x 4 mm) after calibration of the radiograph. **3B.** Classifiers of different sizes were positioned in areas of opposite densities: red classifiers in radiopaque areas – bone and implant surface; green classifiers in radiolucent areas – halo artefact area. **3C.** The segmented halo artefact area (in green) was obtained, in mm².

Statistical analysis

Data collected in the subjective and objective analyses were tabulated in the Microsoft Excel program. The intra-examiner reproducibility values were calculated using the Kappa test (subjective analysis) and the Intraclass Correlation Coefficient (ICC) (objective analysis). The values were interpreted according to Landis and Koch (1977)[16] (subjective analysis) and Szklo and Nieto (2016)[17] (objective analysis).

In the subjective analysis, data consisted of dichotomous nominal variables (presence/absence of halo) and was expressed as the absolute and relative frequency of radiographs with halo per surface and per experimental group. These data were analyzed by Cochran's Q test with pairwise McNemar post-hoc. Data collected in the objective analysis comprised continuous quantitative variables (area of segmented halo, in mm²) and was descriptively presented as the mean and the standard deviation of the segmented halo areas in mm². Since the Shapiro-Wilk and the Barllet tests showed normal distribution and variances, the data were submitted to ANOVA. Statistics were performed considering the paired groups shown in Table 1 using two software programs: R version 4.0.0 (R Foundation for Statistical Computing, Vienna, Austria) and Jamovi version 1.6.3 (The Jamovi Project, Sidney, Australia[18]). The significance level was adopted at 5%.

Results

Intra-examiner reproducibility was substantial for the subjective analysis (Kappa = 0.75) and excellent for the objective analysis (ICC = 0.76). None of the film-based radiographs showed peri-implant radiolucencies.

Table 2 features the absolute and relative frequency of radiographs with halo considering each surface and each experimental group, based on the subjective analysis.

No surface showed statistically significant differences between the paired groups considering halo presence ($p > 0.05$).

Table 2. Absolute and relative frequency of surfaces with halo considering each experimental group, according to the subjective analysis.

Group	Surface		
	Left	Right	Apical
A	7 (29.2%)	5 (20.8%)	9 (37.5%)
B	9 (37.5%)	8 (33.3%)	5 (20.8%)
C	5 (20.8%)	4 (16.7%)	6 (25%)
D	8 (33.3%)	12 (50%)	6 (25%)
E	5 (20.8%)	5 (20.8%)	8 (33.3%)
F	5 (20.8%)	10 (41.7%)	8 (33.3%)
p-value	0.36	0.05	0.26
Total	39 (27.1%)	44 (30.6%)	42 (29.2%)

Group A – low frequency, PSP, 70 kVp; Group B – low frequency, CMOS, 70 kVp; Group C – high frequency, PSP, 70 kVp; Group D – high frequency, CMOS, 70 kVp; Group E – high frequency, PSP, 60 kVp; Group F – high frequency, CMOS, 60 kVp.
* p < 0.05, according to Cochran's Q test.

In the subjective analysis, 85 of 144 radiographs expressed halo artefact on at least one of the surfaces and were included in the objective analysis. The left, right and apical surfaces of all 85 radiographs were objectively assessed. Table 3 shows the number of surfaces with halo and the mean and standard deviation values for the halo segmented areas by surface and experimental group. No surface showed statistically significant differences among the groups considering areas of halo artefact ($p > 0.05$).

Table 3. Number of surfaces with halo and mean and standard deviation of the halo segmented areas (in mm²), considering each surface and each experimental group, according to the objective analysis.

Group	N	Mean (SD), mm² / Surface		
		Left	Right	Apical
A	13	1.093 (0.177)	0.948 (0.192)	1.197 (0.336)
B	15	1.122 (0.267)	0.899 (0.289)	1.090 (0.392)
C	11	1.101 (0.181)	0.925 (0.272)	1.175 (0.251)
D	18	0.981 (0.318)	0.930 (0.239)	1.056 (0.318)
E	13	1.146 (0.224)	0.832 (0.187)	1.307 (0.286)
F	15	0.949 (0.305)	0.864 (0.217)	1.092 (0.312)
p-value		0.346	0.693	0.307

N, number of surfaces with halo; SD, standard deviation; Group A – low frequency, PSP, 70 kVp; Group B – low frequency, CMOS, 70 kVp; Group C – high frequency, PSP, 70 kVp; Group D – high frequency, CMOS, 70 kVp; Group E – high frequency, PSP, 60 kVp; Group F – high frequency, CMOS, 60 kVp.
* p < 0.05, according to ANOVA.

Discussion

In this study, we aimed to assess the influence of the X-ray source and the image receptor on the expression of halo artefacts in digital radiographs of dental implants, since this artefact can simulate failures in the osseointegration of implants[4]. Each factor under study was considered individually by paired group comparisons. To the best of our knowledge, this was the first study to evaluate whether different X-ray sources and radiographic receptors used in dentistry can improve the bone-to-implant interface, avoiding the expression of the halo artefact in terms of presence and magnitude.

We used subjective analysis (presence or absence of halo) and objective analysis (area of halo expressed in mm^2) considering that both could relate to osseointegration diagnosis, since these provided assessment of radiolucent area in the bone-to-implant interface. Kappa and ICC values were above 0.75, indicating substantial and excellent reproducibility for subjective and objective analyses, respectively. Calibration of the examiners was unnecessary since the study did not aim to standardize the diagnosis of artefact but rather to obtain the perception of the two examiners. In the objective assessment, semi-automatic segmentation minimized the possibility of inconsistent responses.

In this study, the file format used was .jpg. Miranda-Viana et al. (2021)[19] observed that digital radiographic images could be stored in different file formats, i.e., TIFF, BMP, PNG and JPEG, without affecting the diagnosis of root resorption. Additionally, Madlum et al. (2021)[20] also observed that the same digital file formats did not influence the radiographic diagnosis of proximal caries lesions.

The electronic components of a CMOS receptor for reading and signal amplification are encapsulated within a plastic casing to protect them from deterioration and contamination at the oral cavity, while making it bulkier[21]. Since this plastic casing is composed of a polymer which presents a low physical density, its interaction with the X-ray beam is not associated with photoelectric absorption but mainly with radiation scattering, i.e. the X-ray beam interacts with the object and the scattered photons still reach the sensor. Radiation scattering reduces the image quality and can generate radiolucent artefacts in digital images[9-11]. However, we did not find any statistically significant differences between the two radiographic receptors, so this effect showed to be insufficient to interfere in the presence and magnitude of the halo artefacts generated.

The artefacts that occur by radiation scattering can be reduced by decreasing kVp and by an accurate collimation of the radiation beam[10]. A previous study found that digital images of humeral implants obtained with the lowest kVp values were less associated with the formation of halo artefacts[22]. Low-energy photons tend to be more absorbed than high-energy photons; for this reason, low kVp values result in more attenuated photons[22], which may decrease scattering radiation and, consequently, the production of radiolucent artefacts. However, we did not find any statistically significant differences between the values of 60 and 70 kVp. It is noteworthy that Hudek et al. (2017)[22] worked with greater kVp variations than those available for periapical X-ray devices such as ours.

The influence of the X-ray source on the formation of halo artefacts in digital radiographs of dental implants has not yet been considered in the literature, to the best of our knowledge. When using high-frequency devices, the anode's voltage varies from zero to the kVp setting, therefore the intensity of radiation tends to be as high as the kVp value, and the beam energy presents less heterogeneity than that produced by low-frequency sources. In addition to energy use[13], high-frequency X-ray machines produce images with a longer contrast scale, i.e., smaller differences between adjacent densities[14]. Thus, we hypothesized that high-frequency X-ray machines could be less associated with halo artefacts, attenuating the abrupt difference of density between dental implant and adjacent bone. Nonetheless, our hypothesis could not be confirmed, since there were no statistically significant differences between the groups considering X-ray sources.

Still, the decrease in image contrast is also related to greater radiation dispersion, which is influenced by the increase in kVp, as shown above. In addition, Compton scattering is favored when using higher kVp and lower mAs (milliamperage x exposure time in seconds)[13]. Both devices used herein have a constant milliamperage factor. Furthermore, since this is an *ex-vivo* study that aimed to analyze isolated study factors, the exposure time parameter was standardized for all radiographs. Thus, the time used may have been a factor that influenced our results when considering that, in clinical conditions, the devices would need different exposure times because they have different generators.

The *ex vivo* model has some inherent limitations that could be overcome in an *in vivo* study. In order to enable comparison between digital receptors, X-ray sources and kVp values, it was necessary to standardize the sample. Thus, to avoid repeated exposure of patients to X radiation, the use of a human jaw with installed implants and an acrylic plate to simulate soft tissues attenuation were the selected model to mimic a clinical condition, preserving the ethical integrity of this study. Future studies may involve analysis of the presence of the halo artefact in periapical radiographs taken from patients for clinical purposes. In addition, a dichotomy analysis might be considered as a method that could overlook tenuous effects of the halo artefact. Initially, we proposed a 3-point scale; however, we observed that only two scores were chosen during image analysis, i.e., the expression of halo artefact was only considered as present or not present. Further studies should continue exploring the subject employing other quantitative methods, such as image subtraction.

At last, we understand that brightness and contrast adjustments and filter application are features commonly used in a clinical context. Nevertheless, these adjustments were not allowed during image evaluation, since they modify the image grey values[23]. Sharpening filters enhance high frequency image content and reduce low frequency ones, intensifying image contrast and highlighting structure boundaries[24,25], and increase image noise[25]. Thus, we consider that these adjustments could possibly influence the expression of halo artefacts, and next studies shall be developed assessing their impact on halo artefacts.

In conclusion, the presence and magnitude of halo artefacts did not differ according to the image receptor and the X-ray source, considering the ones tested in the present study. Future studies are still needed to clarify our findings.

Disclosures

Funding

The authors thank Conselho Nacional de Desenvolvimento Científico e Tecnológico and Coordenação de Aperfeiçoamento de Pessoal de Nível Superior (Finance Code 001) for the scholarships granted to Manuella Soussa Braga and Fernanda Coelho Silva, respectively. The authors are also thankful to the Fundação de Amparo à Pesquisa e Inovação do Espírito Santo – FAPES (007/2014 and 22/2018) for providing the X-ray device used in this research.

Data Availability

Datasets related to this article will be available upon request to the corresponding author.

Declarations of interest

The authors declare openly that there are no conflicts of interest in relation with this article.

Author Contribution

All authors actively participated in discussing the manuscript's findings and have revised and approved the final version of the manuscript. **Manuella Soussa Braga**: Investigation (lead); Writing – original draft (lead); Visualization (equal); Methodology (equal); Conceptualization (equal); Funding acquisition (equal). **Ana Maria de Almeida Ramos:** Investigation (equal); Methodology (equal); Conceptualization (equal); Writing – original draft (supporting); Funding acquisition (supporting). **Fernanda Coelho-Silva**: Writing – review & editing (lead); Formal analysis (equal); Visualization (equal); Writing – original draft (equal); Data curation (equal); Conceptualization (supporting); Validation (supporting); Supervision (supporting). **Teresa Cristina Rangel Pereira:** Project administration (lead); Funding acquisition (lead); Conceptualization (equal); Supervision (equal); Resources (equal); Methodology (equal); Writing – review & editing (supporting). **Sergio Lins de-Azevedo-Vaz**: Conceptualization (lead); Methodology (lead); Validation (lead); Formal analysis (lead); Data curation (lead); Supervision (lead); Resources (lead); Writing – review & editing (equal); Project administration (equal); Funding acquisition (equal).

References

1. Albrektsson T, Zarb G, Worthington P, Eriksson AR. The long-term efficacy of currently used dental implants: a review and proposed criteria of success. Int J Oral Maxillofac Implants. 1986 Summer;1(1):11-25.

2. Wenzel A, Møystad A. Work flow with digital intraoral radiography: a systematic review. Acta Odontol Scand. 2010 Mar;68(2):106-14. doi: 10.3109/00016350903514426.

3. Ajmal M, Elshinawy MI. Subjective image quality comparison between two digital dental radiographic systems and conventional dental film. Saudi Dent J. 2014 Oct;26(4):145-50. doi: 10.1016/j.sdentj.2014.05.007.

4. Brettle D, Carmichael F. The impact of digital image processing artefacts mimicking pathological features associated with restorations. Br Dent J. 2011 Aug;211(4):167-70. doi: 10.1038/sj.bdj.2011.676.

5. Tan TH, Boothroyd AE. Uberschwinger artefact in computed radiographs. Br J Radiol. 1997 Apr;70(832):431. doi: 10.1259/bjr.70.832.9166087.

6. Clark JL, Wadhwani CP, Abramovitch K, Rice DD, Kattadiyil MT. Effect of image sharpening on radiographic image quality. J Prosthet Dent. 2018 Dec;120(6):927-933. doi: 10.1016/j.prosdent.2018.03.034.

7. Schweitzer DM, Berg RW. A digital radiographic artifact: A clinical report. J Prosthet Dent. 2010 Jun;103(6):326-9. doi: 10.1016/S0022-3913(10)00082-X.

8. Yoshida M, Yoshihara H, Honda E. History of digital detectors in intraoral radiography. Dent Health Curr Res. 2018;4(2):1-5. doi: 10.4172/2470-0886.1000135.

9. Farias Gomes A, Nejaim Y, Fontenele RC, Haiter-Neto F, Freitas DQ. Influence of the incorporation of a lead foil to intraoral digital receptors on the image quality and root fracture diagnosis. Dentomaxillofac Radiol. 2019 Sep;48(6):20180369. doi: 10.1259/dmfr.20180369.

10. Solomon SL, Jost RG, Glazer HS, Sagel SS, Anderson DJ, Molina PL. Artifacts in computed radiography. AJR Am J Roentgenol. 1991 Jul;157(1):181-5. doi: 10.2214/ajr.157.1.2048517.

11. Shetty CM, Barthur A, Kambadakone A, Narayanan N, Kv R. Computed radiography image artifacts revisited. AJR Am J Roentgenol. 2011 Jan;196(1):W37-47. doi: 10.2214/AJR.10.5563.

12. Helmrot E, Matscheko G, Carlsson GA, Eckerdal O, Ericson S. Image contrast using high frequency and half-wave rectified dental x-ray generators. Dentomaxillofac Radiol. 1988;17(1):33-40. doi: 10.1259/dmfr.1988.0004.

13. Machado DRL. [Physics applied to radiology]. Indaial: Uniasselvi; 2019. Portuguese.

14. Barthez PY, Manwaring N, Mitelmann PH, Benoit E. Comparison of single-phase and high-frequency generators for x-ray units. Vet Radiol Ultrasound. 2002 Mar-Apr;43(2):118-22. doi: 10.1111/j.1740-8261.2002.tb01658.x.

15. Cançado Oliveira BF, Valerio CS, Jansen WC, Zenóbio EG, Manzi FR. Accuracy of digital versus conventional periapical radiographs to detect misfit at the implant-abutment interface. Int J Oral Maxillofac Implants. 2016 Sep-Oct;31(5):1023-9. doi: 10.11607/jomi.4525.

16. Landis JR, Koch GG. The measurement of observer agreement for categorical data. Biometrics. 1977 Mar;33(1):159-74.

17. Szklo M, Nieto FJ. Epidemiology: Beyond the Basics. 3rd ed. Burlington: Jones & Bartlett Publishers; 2016.

18. The jamovi project (2020). jamovi. (Version 1.2) [Computer Software]. Available from https://www.jamovi.org.

19. Miranda-Viana M, Madlum DV, Oliveira-Santos N, Gaêta-Araujo H, Haiter-Neto F, Oliveira ML. Influence of the image file format of digital periapical radiographs on the diagnosis of external and internal root resorptions. Clin Oral Investig. 2021 Aug;25(8):4941-8. doi: 10.1007/s00784-021-03803-0.

20. Madlum DV, Gaêta-Araujo H, Brasil DM, Lima CAS, Oliveira ML, Haiter-Neto F. Influence of the file format and transmission app on the radiographic diagnosis of caries lesions. Oral Surg Oral Med Oral Pathol Oral Radiol. 2021 Oct;132(4):448-55. doi: 10.1016/j.oooo.2020.11.013. Epub 2020 Dec 8.

21. Haiter Neto F, Melo DPD. [Digital radiography]. Rev ABRO. 2010;11(1):5-17. Portuguese.

22. Hudek R, Werner B, Abdelkawi AF, Schmitt R, Gohlke F. Radiolucency in stemless shoulder arthroplasty is associated with an imaging phenomenon. J Orthop Res. 2017 Sep;35(9):2040-50. doi: 10.1002/jor.23478.

23. Suetens P. Fundamentals of medical imaging. 2nd ed. Cambridge: Cambridge University Press; 2009.

24. Mouzinho-Machado S, Rosado LPL, Coelho-Silva F, Neves FS, Haiter-Neto F, de-Azevedo-Vaz SL. Influence of voxel size and filter application in detecting second mesiobuccal canals in cone-beam computed tomographic images. J Endod. 2021 Sep;47(9):1391-7. doi: 10.1016/j.joen.2021.06.011.

25. Gaêta-Araujo H, Nascimento EHL, Oliveira-Santos N, Queiroz PM, Oliveira ML, Freitas DQ, et al. Effect of digital enhancement on the radiographic assessment of vertical root fractures in the presence of different intracanal materials: an in vitro study. Clin Oral Investig. 2021 Jan;25(1):195-202. doi: 10.1007/s00784-020-03353-x. Epub 2020 Jun 6.